Spatial Phase shifting in ESPI:
Influence of second-order Speckle Statistics on Fringe Quality

J. Burke, T. Bothe, H. Helmers, C. Kunze, R. S. Sirohi, V. Wilkens
Carl von Ossietzky Universität Oldenburg, FB Physik, Postfach 2503, D-26111 Oldenburg

1. Introduction

The advent of phase shifting has greatly enhanced the capabilities of ESPI /1, 2/. However, temporal phase shifting (TPS) is not well suited for tasks where random time-dependent phase fluctuations between the phase-shifted frames, as caused by vibration, air turbulence, or rapid object motion, can spoil the measurement.

The solution to these problems is the complementary technique, spatial phase shifting (SPS) /3/, where the phase is not shifted in time but in one spatial direction, as shown in Fig. 1. A conventional ESPI setup is modified by shifting the origin of the reference wave by Δx from the center of the aperture; this generates a linear phase shift $\beta(\Delta x)$ on the sensor. Thus the phase shifted frames can be recorded simultaneously and time-dependent errors are excluded.

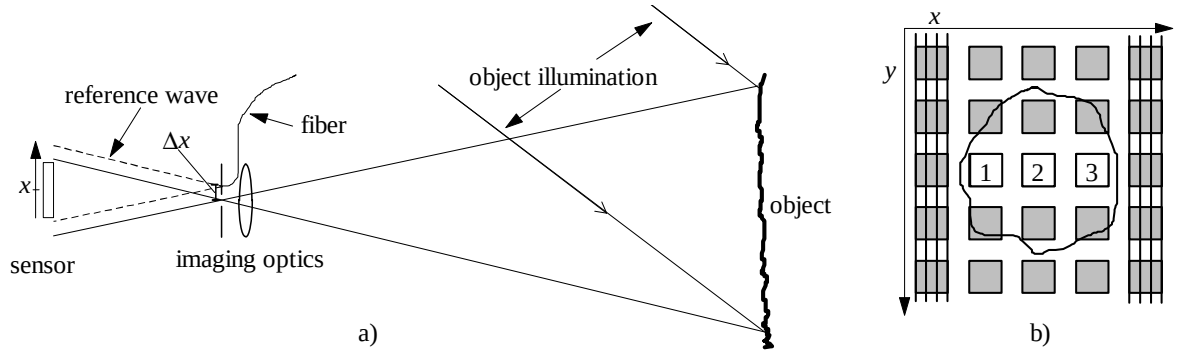

Fig. 1: a) ESPI setup modified for SPS; b) arrangement of measuring points 1,2,3 within the correlation area; line arrays indicate orientation and spacing of carrier fringes (phase shift set to $\pi/2$).

However, SPS has some drawbacks to cope with in ESPI. In most phase reconstruction formulas, intensity and phase of the object wave are assumed to be constant for all measurements entering the phase calculation together. In TPS where pointwise data sets each stem from the same location, this is fully justified as long as temporal parameter fluctuations can be avoided. The data sets for SPS however are made up of adjacent pixels as indicated in Fig. 1 b) and the speckle size must be increased to keep the pixels within one correlation cell (i.e. speckle size). Even so, the spatial intensity and phase gradients of the object's speckle pattern introduce severe errors in the phase reconstruction. The smaller the mean speckle size is chosen, the larger the random noise in the reconstructed phase map will be. On the other hand, enlarging the speckles implies losing object light and spatial resolution.

The latter is not a problem in ESPI where lowpass filtering is usual. Concerning the former however, it is desirable to tailor phase retrieval schemes for SPS that permit to keep the speckles as small as possible while delivering acceptable results. This paper reports on improvements in the phase reconstruction out of spatially phase shifted speckle interferograms. First a brief overview of second-order speckle statistics is given; then algorithms for improved phase calculation are developed. We also introduce a method of phase shifting that allows for multiple phase measurements at each point and finally compare the merits of each approach.

2. Second-order speckle statistics

The spatial coherence of two different locations in a speckle field determines the probability of intensity and/or phase deviations between them /4/. The probability density functions of speckle intensity gradients and phase gradients, respectively, have been derived in /5/ and /6/. The conditional pdf's for intensity and phase given in /4/ have been extended /7/ to involve four quantities: I_1 and φ_1, intensity and phase at the first point of interest, and I_2, φ_2 for the second point. All of these are interrelated so that neither intensity nor phase may be considered alone.

The conclusion of these studies is that high phase gradients are likely to occur in dark regions of the speckle pattern, becoming infinite in the immediate vicinity of the 'screw dislocations' /8, 9/ appearing at the points of zero amplitude. In contrast, the phase tends to vary more slowly in the bright parts of the speckle field (i.e., the speckle spots). These facts can intuitively be understood in the phasor representation. Fig. 2 gives an impression of the spatial distribution of intensities and phases in speckle patterns. The speckle size was about 45 pixels and the phase was measured by SPS.

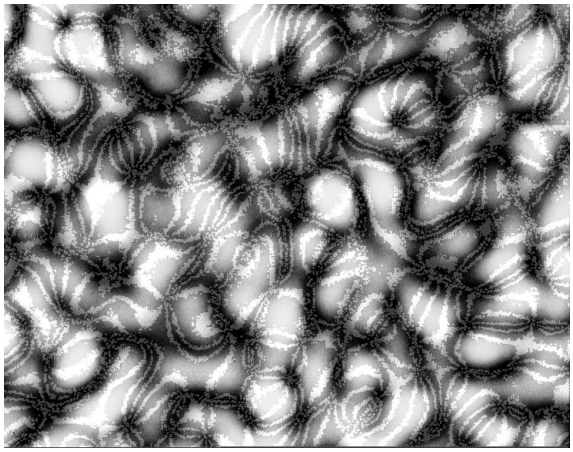

Fig. 2: Speckle intensities and phases (overlaid isolines) of an actual speckle pattern.

Recently there has been some interesting work that presents the statistics in a highly useful manner. According to /10/, the mean phase gradient in the centers of speckle spots is about 50° per speckle diameter: This is not to say that the phase variation in a speckle never exceeds that value; even higher gradients can occur.

Hence there are good reasons to account for the speckle structure of SPS data in the phase evaluation. Firstly, we find high intensity gradients at the edges of the speckle spots /11/, spoiling data sets at those locations. Secondly, the often made assumption of constant speckle phase does not hold well enough when SPS is considered.

3. Computational methods for error reduction

3.1 Incorporation of object intensity

In order to limit the loss of collected light, we restrict ourselves to the smallest possible number of measurement points, which is three. Accordingly, the mean speckle size is 19 μm (2.5 pixel distances) for all measurements shown in this paper. Superposing a reference to the object wave and introducing the phase shift ($\pi/2$ throughout the experiments), the resulting irradiance in sensor column $(n+m)$ is given by

$$I_{n+m} = I_0 \left(1 + \gamma \ \mathrm{sinc}\left(\frac{\Phi}{2} \right) \cos(\varphi_n + n\beta + m\beta + C) \right) \qquad (1)$$

(n= 2,...,M-1 (M: column count of camera), m= -1, 0, 1; I_0: mean intensity, β: phase shift per column, γ: visibility, Φ: phase angle over which the pixels integrate the intensity, C: phase offset, y-dependency omitted for clarity). For finding φ_n , we insert the pixel at nth place plus its left and right neighbor pixels, phase shifted by -β and β, respectively, into the usual phase reconstruction formula:

$$\varphi_n \bmod \pi = \tan^{-1}\left(\frac{1-\cos\beta}{\sin\beta}\cdot\frac{I_{n-1}-I_{n+1}}{2I_n-I_{n-1}-I_{n+1}}\right). \qquad (2)$$

Thus, each interferogram yields a speckle phase map. Acquiring phase maps φ_{n1} before and φ_{n2} after a displacement and subtracting them gives the displacement map or sawtooth image of $\Delta\varphi_n$. Throughout section 3 always the same couple of interferograms was used for evaluation. The displacement measured was the out-of-plane tilt of a flat plate.

It is possible to account for the non-constancy of I_0 and γif (1) is rewritten as

$$I_{n+m} = O_{n+m} + R + 2\sqrt{O_{n+m}\cdot R}\ \mathrm{sinc}\left(\frac{\Phi}{2}\right)\cos(\varphi_n + n\beta + m\beta + C); \qquad (3)$$

O_{n+m}: intensity in the speckle field of the object wave alone at the (n+m)th column, R : intensity of the reference wave. R is assumed spatially constant. O_{n+m} must be recorded before – and in the case of speckle decorrelation, also after – the acquisition of the interferograms $I_{(n+m)1}$ and $I_{(n+m)2}$.

With the modified interferogram equations, the phase reconstruction formula (2) changes to

$$\varphi_n \bmod \pi = \tan^{-1}\frac{\sqrt{O_n}(D_{n-1}-D_{n+1}) - \cos\beta\left(\sqrt{O_{n-1}}(D_n-D_{n+1}) + \sqrt{O_{n+1}}(D_{n-1}-D_n)\right)}{\sin\beta\left(\sqrt{O_{n-1}}(D_n-D_{n+1}) - \sqrt{O_{n+1}}(D_{n-1}-D_n)\right)} \qquad (4)$$

with D_n=I_n-O_n /12/. Fig. 3 compares the approaches of eqs. 2 and 4. A quantification of the improvement yielded about 19% less noise in phase map b) than in a).

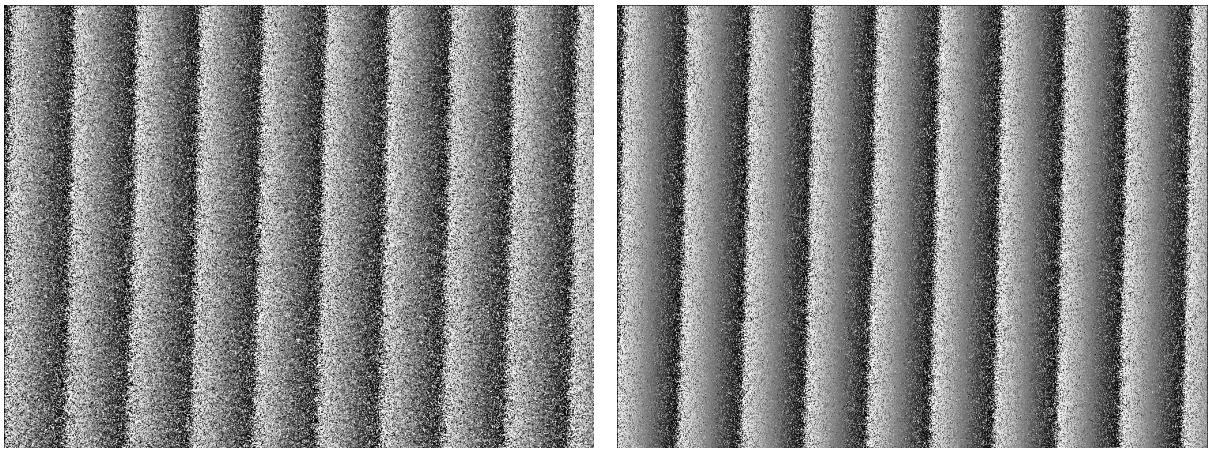

a) b)

Fig. 3: Results of phase calculations; a) with eq. 2, b) with eq. 4.

3.2 Correction of varying speckle phase

As the phases of speckles of the size used here cannot be measured with sufficient resolution, the simple assumption is made that not the phase, but the phase gradient be constant over the adjacent pixels used. (The interested reader may check this in Fig. 2.) This is equivalent to local linear deviations of the phase shift from its nominal value. The problem of linear phase

shifting errors has been treated extensively in TPS research and there are many compensating algorithms. Provided the phase shift is set to π/2, we may use a 3+3 averaging algorithm as described in /13/:

$$\varphi_n \mod \pi = \tan^{-1} \frac{2(I_n - I_{n+1})}{I_{n-1} - I_n - I_{n+1} + I_{n+2}}. \tag{5}$$

This algorithm uses four intensity readings and seemingly forces the speckle size to be further increased. It was observed, however, that the phase map even benefits from the lowpass characteristic of the formula when the speckle size is maintained. This can be seen in Fig. 4 a); the noise is reduced by approx. 7% compared to Fig. 3 a). No spatial resolution is lost here as the speckles have been enlarged anyway.

3.3 Combination of intensity and phase correction

The simplest way to construct a phase calculation that corrects errors by both intensity and phase gradients is to establish an averaging algorithm for terms in the form of (4). For $\beta=\pi/2$, (4) becomes

$$\varphi_n \mod \pi = \tan^{-1} \frac{\sqrt{O_n}(D_{n-1} - D_{n+1})}{\sqrt{O_{n-1}}(D_n - D_{n+1}) - \sqrt{O_{n+1}}(D_{n-1} - D_n)} := \frac{K_1}{K_2 - K_3}, \tag{6}$$

and shifting the pixel triplet by one position yields

$$\varphi_{n+1} \mod \pi = \tan^{-1} \frac{\sqrt{O_{n+1}}(D_n - D_{n+2})}{\sqrt{O_n}(D_{n+1} - D_{n+2}) - \sqrt{O_{n+2}}(D_n - D_{n+1})} := \frac{K_4}{K_5 - K_6}. \tag{7}$$

The phase is now simply calculated by

$$\varphi_n \mod \pi = \tan^{-1} \frac{K_1 + K_4}{K_2 + K_5 - K_3 - K_6} \tag{8}$$

so that the new φ_n is the mean of the old φ_n and φ_{n+1}. It is worth noting that this manner of averaging works properly only for the phase shift of π/2. The resulting phase map is shown in Fig.4 b) and shows about 27% less noise than that of Fig. 3 a).

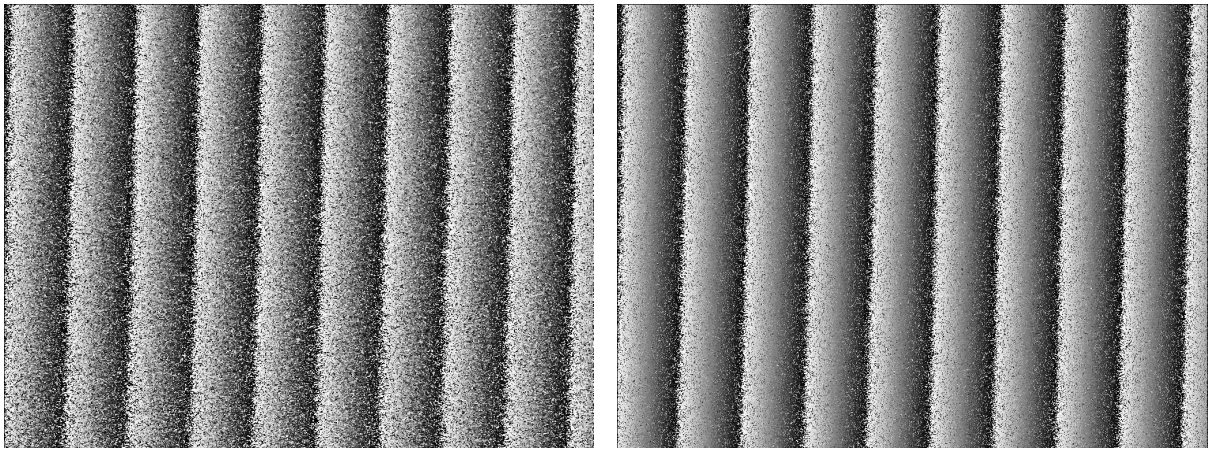

a) b)

Fig. 4: a) phase calculation with eq. 5; b) phase calculation with eq. 8.

4. Experimental method for error reduction

If the measuring points are arranged as in Fig. 1 b) and the phase shift is in x-direction only, the vertical extent of the correlation area is not made use of. Setting the speckle dimensions to 3x1 pixels as advisable from the standpoint of light efficiency is ruled out because of the significant increase of noise. If however a full-frame camera is available, all image lines can be acquired simultaneously. Hence it is possible to add $\beta(\Delta y)$, resulting in a tilt of the carrier fringes and allowing to arrange the set of pixels used in *y*- or any desired direction. This enables the speckle shape to be fully exploited for measurement. Fig. 5 shows a direction and spatial frequency for the carrier fringes that permits arranging the pixels evaluated in various ways. This can first be seen in Fig. 5 a) where eq. 4 may work both in x- and y-direction . It is also possible to obtain phase values from the pixel clusters shown in Fig. 5 b), resulting in two additional measurements for the central pixel. The phase maps thus obtained show higher noise than those out of pure x- and y-directions: although the nominal phase shifts are correct, the pixels involved are not on a straight line. However, taking as phase value the arithmetic mean of all four measurements still leads to an improvement over the x- and y-measurements alone. The result of the former is displayed in Fig. 6 a). Here we get a noise reduction of about 26% compared to Fig. 3 a), necessarily with different interferograms but all experimental parameters unchanged, except for the carrier fringe orientation.

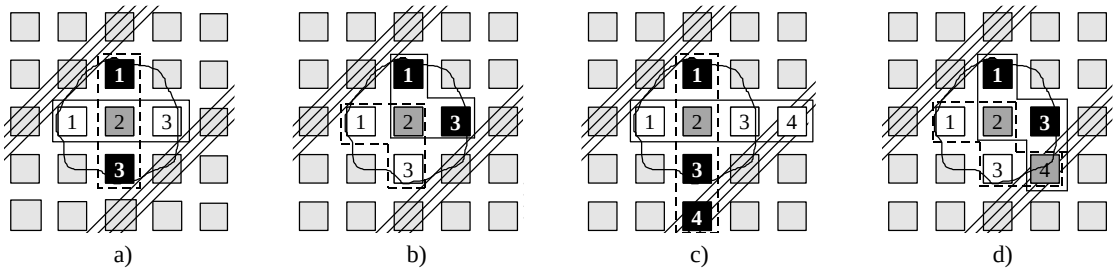

Fig. 5: Various pixel clusters for phase calculation. Grouping indicated by outlines and black/white colour; pixels used twice are dark grey. a) and b): double 3-point arrangement; c) and d): double 3+3-point arrangement.

The 3+3 algorithm as in (8) can be used for phase retrieval in the configuration of Fig. 5 c). According to Fig. 5 d), additional sets of points can be obtained as well and the average of them all indeed yields the best phase map obtained so far, which can be seen in Fig. 6 b). The noise there is by about 33% lower than in Fig. 3 a).

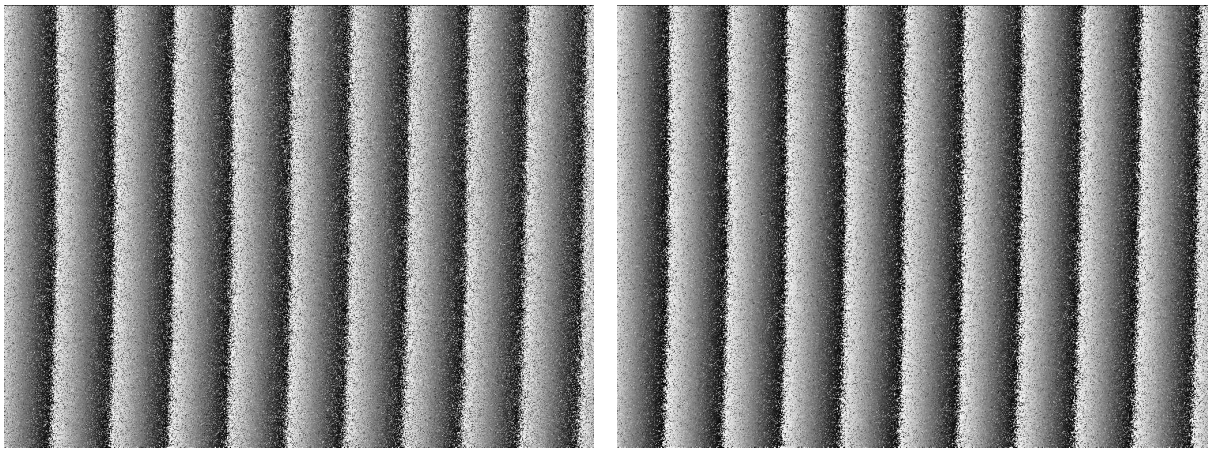

Fig. 6: Phase maps resulting from fourfold phase determination at each point; a) measurements as in Fig. 5 a) and b) averaged; b) measurements as in Fig. 5 c) and d) averaged.

5. Conclusions

Some phase retrieval methods specially adapted to SPS are presented. A 3-point algorithm accounting for the object's speckle intensities is proposed; moreover, a well-known averaging technique is utilized to suppress errors by speckle phase gradients. For the measuring process a phase shift direction is suggested that permits multiple phase measurements for any point in the interferogram. The approaches are tested separately and together. The inclusion of the object intensities into the calculation turns out to effect remarkable improvement in the calculated phase maps; however this requires additional recording of at least one speckle image of the object. The correction for phase shift errors due to speckle phase gradients contributes a smaller part to noise suppression. The averaging of multiple measurements also reduces the noise noticeably; here the possibilities are not yet exploited as one might incorporate a suitable weighting scheme for the phase values obtained, yet probably at the cost of computational simplicity. It is seen that some of the new algorithms outperform the old one distinctly.

6. Acknowledgements

J. Burke gratefully acknowledges financial support of the Deutsche Forschungsgemeinschaft, DFG. R.S. Sirohi would like to thank the Alexander von Humboldt Foundation Germany for the award of the Humboldt Research award to enable him to spend a year in Germany.

7. References

/1/ Nakadate, S., and Saito, H., Fringe scanning speckle-pattern interferometry. Appl. Opt. 24(1985)14, 2172-2180

/2/ Creath, K.: Phase shifting speckle interferometry. Appl. Opt. 24(1985)18, 3053-3058

/3/ Gutjahr, J.:New developments in phase shifting interferometry. Proc. Fringe '93, ed. by W. Jüptner and W. Osten; Akademie Verlag, Berlin (1993), 60-65

/4/ Goodman, J. W.: Statistical properties of laser speckle patterns. in: Laser Speckle and related Phenomena, ed. by J.C. Dainty. Springer-Verlag, Berlin (1984), 35-46

/5/ Ebeling, K. J.: Statistical properties of spatial derivatives of the amplitude and intensity of monochromatic speckle patterns. Opt. Act. 26(1979), 1505-1521

/6/ Ochoa, E., and Goodman, J. W.: Statistical properties of ray directions in a monochromatic speckle pattern. J. Opt. Soc. Am. 73(1983)7, 943-949

/7/ Donati, S., and Martini, G.: Speckle-pattern intensity and phase: second-order conditional statistics. J. Opt. Soc. Am. 69(1979)12, 1690-1694

/8/ Berry. M. V.: Disruption of wavefronts: statistics of dislocations in incoherent Gaussian random waves, J. Phys. A 11(1978)1, 27-37

/9/ Baranova, N. B., et al.: Wave-front dislocations: topological limitations for adaptive systems with phase conjugation. J. Opt. Soc. Am. 73(1983)5, 525-528

/10/ Shvartsman, N., and Freund, I.: Speckle spots ride phase saddles sidesaddle. Opt. Comm. 117(1995), 228-234

/11/ Freund, I.: Intensity critical point correlation functions in random wave fields. Opt. Comm 128(1996) 315-324, and references therein

/12/ Bothe, T., Burke, J., et al.: Spatial phase shifting in ESPI: minimization of phase reconstruction errors. Appl. Opt, in press.

/13/ Schwider, J., et al.: New compensating four-phase algorithm for phase-shift interferometry. Opt. Eng. 32(1993)8, 1883-1885